Chapter

Hard Pure-Gold and Gold-CNT Composite Plating Using Electrodeposition Technique with Environmentally Friendly Sulfite Bath

Masatsugu Fujishige and Susumu Arai

Abstract

Gold was used by Chinese and Egyptians of ancient times (at least ca 3000 BC). For many years, gold based materials have received great attention from people, due to the good conductor, high chemical stability, unique optical and processable properties. Electrodeposition technology is a long established technique for synthesizing metals on conductive substrates. Advances in equipment and creations of nanomaterials could carry out new technological progress, a large duty ratio with a pulse overvoltage became possible and new composite fillers (for example, carbon nanotubes: CNTs) appeared. Moreover, environmental considerations have become more important as Sustainable Development Goals (SDGs). SDGs were adopted at the United Nations Summit in September 2015 and are the goals set by the 193 member countries to achieve in the 15 years from 2016 to 2030. For the global environment and workers, friendly manufacturing methods have become more important. In this chapter, two nanostructured golds (hard pure-gold plating and gold-CNT composite plating) are discussed. They are a method of hardening the metal as pure-gold by pulsed electrodeposition and a method of combining CNT by controlling the zeta potential with additives, and their application as a contact material was investigated. Additionally, the synthesis and characteristics of electrostatic deposition films with properties using environmentally friendly sulfite bath are discussed.

Keywords: nanostructure, gold-plating, non-cyanide, Hall-Petch relation, contact resistance, CNT composite

1. Introduction

Richard P. Feynman spoke "There is Plenty of Room at the Bottom" [1]. This talk is given on 26 December 1959, at the annual meeting of the American Physical Society (APS) at the California Institute of Technology, reconsidered the importance and possibility of micro and nanotechnology in recent years. Microelectromechanical systems (MEMS) shows sensors and devices fabricated based on semiconductor microfabrication technology [2]. MEMS are usually used in pressure

sensors, inkjet printers, microfluidics, etc. In recent years, product integration has increased, various problems are occurring. Electric contacts are also no exception, and here we discuss new gold plating that provides a solution to the problem. It is widely used as a contact material.

Gold was used by Chinese and Egyptians of ancient times (at least ca 3000 BC) [3–5]. For many years, gold based materials have received great attention from people, due to the good conductor, high chemical stability, unique optical and processable properties [6]. Electrodeposition technology is a long established technique for synthesizing metals on conductive substrates. The properties of the deposited film are simply controlled by their morphologies (grain size, shape, roughness, brightness). Moreover, the deposited structure depends on process parameters such as the composition, temperature and pH of electrolyte, the magnitude of applied current densities, substrate. Advances in equipment and creations of nanomaterials could carry out new technological progress, a large duty ratio with a pulse overvoltage became possible and new composite fillers (for example, carbon nanotubes: CNTs) appeared. Moreover, environmental considerations have become more important as Sustainable Development Goals (SDGs). SDGs were adopted at the United Nations Summit in September 2015 and are the goals set by the 193 member countries to achieve in the 15 years from 2016 to 2030. For the global environment and workers, friendly manufacturing methods have become more important.

In this chapter, two nanostructured golds (hard pure-gold plating and gold-CNT composite plating) are discussed. Additionally, the synthesis and characteristics of electrostatic deposition films with properties using environmentally friendly sulfite bath are discussed.

2. Two kinds of new gold plating for contact material

2.1 Hard pure-gold plating

In recent years, there has been a demand for miniaturization to various parts due to an increase in degree of integration of electronic parts. Electric signal probes for inspecting semiconductor package parts have the same demand, and the terminal pitch is gradually narrowed. As a result, the mechanical contact pressure of the probe was lowered and its contact resistance increased. Technical problems have been occurred such as the device stability, and heat generation of the electrical contacts for inspecting the electronic parts. For example, at a contact pressure of about 0.5 N, the contact resistance of the probe is 30 mΩ, whereas at a contact pressure of about 0.15 N, the contact resistance reaches 100 mΩ. This Joule heating value is approximately three times as high as the original. Therefore, there is a demand for a new plating film on the probe surface which does not increase the contact resistance even with a low contact force, while maintaining the environment/durability equal to or higher than the conventional level.

Generally, the gold used as the contact point is a soft metal. However, gold plating for inspection probes has a moderate hardness and durability improved by adding trace amount of Co. In this conventional gold plating film, the specific resistance value is higher than that of pure gold, and the contact resistance associated with this value is also increased. Therefore, we focused on hard pure-gold plating technique without alloying [7]. There are reports [8–10] that can control the grain size toward small by pulse plating that repeats ON/OFF of current. The plating bath and the pulse electrodeposition method were devised to decrease the crystal size. In metals, according to Hall-Petch law [6, 11], metals are hardened by

reducing crystal size. The obtained hard pure-gold plating film was applied to the probe surface [12] and its electrical contact characteristics were evaluated. Furthermore, in consideration of recent SDGs correspondence, the non-cyanide base bath has been used for a friendly environmental society.

2.1.1 Material and method

There is a report [13] in which a sulfite complex is used for a non-cyanic plating bath. In this section, the base sulfite bath was used as a non-cyan gold plating bath. **Table 1** shows the composition of the plating bath and the plating conditions.

The condition of rectangular pulse current was optimized at the average current density of 50 A/m^2, the pulse period of 100 ms, and the duty ratio of 0.1. The Ni-P plated film was used as an experimental substrate (amorphous alloy as a base film) with thickness of about 3 μm on Cu plate. A plating bath manufactured by Meltex was used for plating the base film. The substrate used for the experiment was insulated with a masking tape excepting the deposition surface (10 mm × 20 mm), alkaline degreasing and acid treatment were carried out as plating pretreatment. Further, for comparison, a hard gold plating film with Co-content was similarly prepared, which was plated on the probe, used a commercially cyan bath (by Meltex: Auronal 44 BC). The characteristics of the plated films were evaluated in terms of surface morphology, Vickers hardness, X-ray diffraction (XRD), and specific resistance value, by a field emission scanning electron microscope (FE-SEM: S-4100, Hitachi), a dynamic indentation tester (DUH-201, SHIMADZU), X-ray diffractometer (RINT2200V, Rigaku), a four probe method, respectively.

2.1.2 Prototype probe

Figure 1 shows the photograph of the probe with both ends moved (spring movable stroke of 0.65 mm). A prototype was fabricated by plating the developed plating film on the movable part at both ends of the probe (Cu alloy, and the Ni-P plating as base) shown in **Figure 1**.

The repeated durability of the contact resistance was compared and evaluated for the prototype probes (using the same parts) of the current plating film and the developed plating film. Both gold plates were used for the contact resistance measurement of the probe, and a four-terminal method was used for the electric circuit

Sodium gold sulfite	0.05 M
Sodium sulfite	0.5 M
2,2′-bipyridyl	100 ppm
Additive	Small quantity
Bath temperature	60°C
Bath volume	100 ml
Average current density	50 A/m^2
Film thickness	5 μm (efficiency 100%)
Substrate	Amorphous Ni-P alloy film
Anode	Pt-plated Ti mesh
Agitation	Magnetic stirring

Table 1.
Sulfite gold plating bath composition and plating condition.

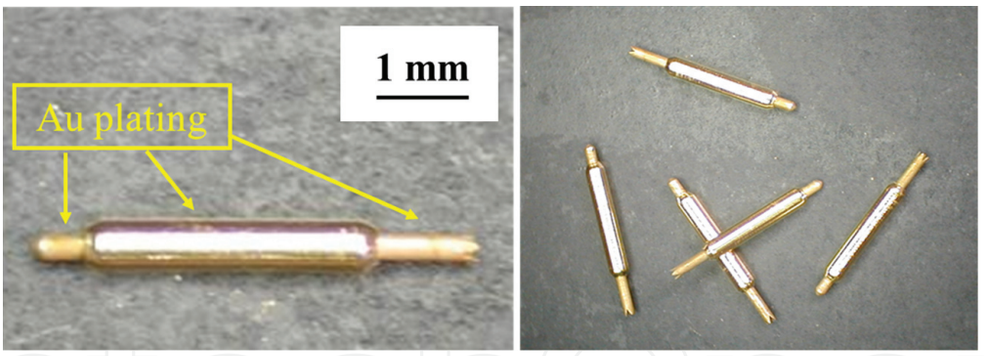

Figure 1.
Photograph of the probe with both ends moved (spring movable stroke of 0.65 mm).

measurement. Here, the measurement was performed at room temperature (RT, the temperature: 24°C, the humidity: 50% [14]) with the probe stroke of 0.65 mm, the load of about 0.24 N, and the measuring current of 10 mA.

2.1.3 Surface observation by FE-SEM

The three types of electrodeposited films, (a) a hard gold plating film with Co-containing (AuCo film) from a cyanide bath, (b) a direct current (DC) gold plating film (DC-Au film) from an original sulfite bath, (c) a pulsed current plating film from the same original sulfite bath (PC-Au film), were prepared and observed the surface morphology by FE-SEM are shown in **Figure 2**, respectively.

Compared with the surface morphology of AuCo film from **Figure 2(a)**, it can be confirmed that the DC-Au film has larger angular crystals (**Figure 2(b)**). The surface of PC-Au film (**Figure 2(c)**) shows the small crystals without corners by comparing with that of DC-Au film (**Figure 2(b)**).

2.1.4 Vickers hardness (Hv) measurement

Figure 3 shows the average value, the maximum value, and the minimum value of Hv obtained from three kinds of plated film surfaces by measuring 10 times at RT using a dynamic indentation tester. Here, the measurement conditions using a diamond indenter were carried out at the test load of 10 gf, the load speed of 0.675 gf/s, and the holding time of 20 s.

From this result, (c) PC-Au film is about twice as hard as (b) DC-Au film, which is harder. The Hv value is close to that of commercially available (a) AuCo film. It is presumed that the improved hardness of PC-Au film is due to the crystal size. Next, the crystal structure of the plating film was investigated by XRD.

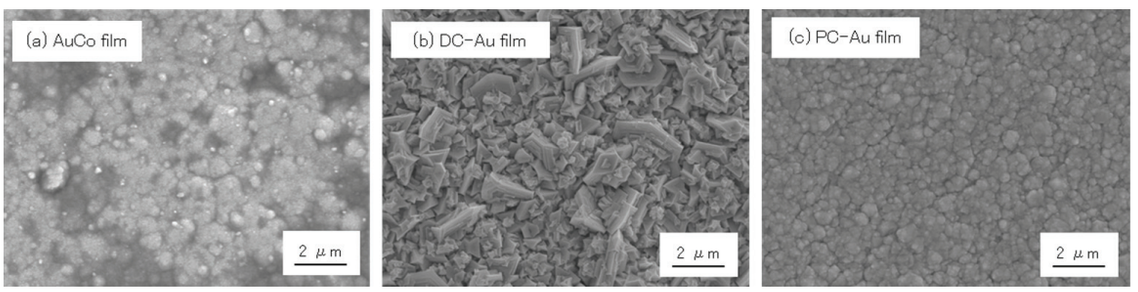

Figure 2.
Surface SEM images of various Au plating films, (a) AuCo film, (b) DC-Au film, (c) PC-Au film.

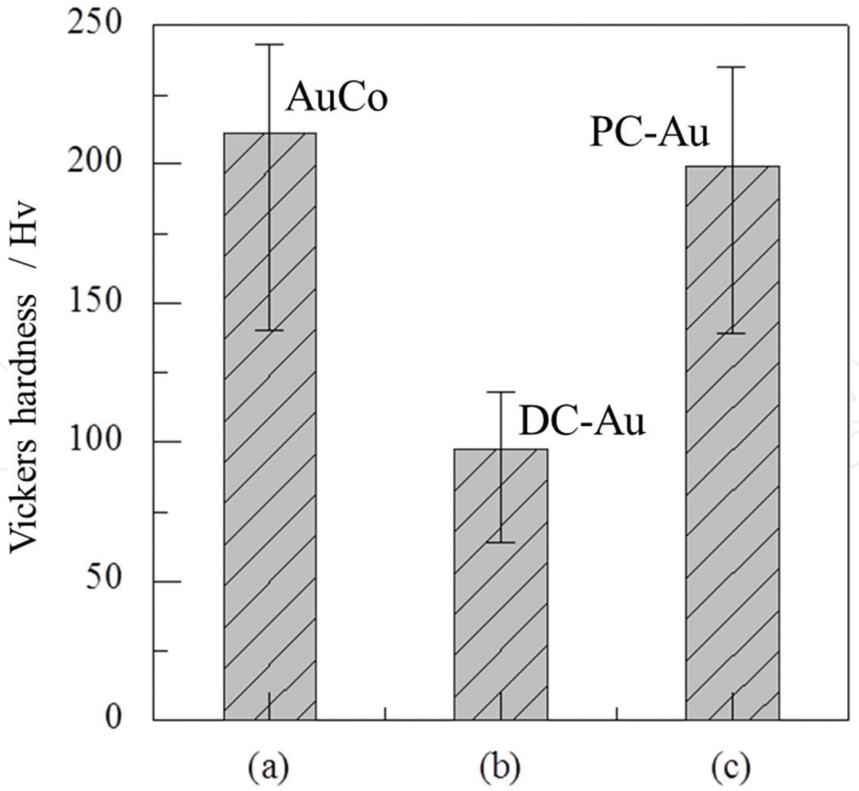

Figure 3.
Vickers hardness (the average, maximum and minimum value) of various Au plating films; (a) AuCo film, (b) DC-Au film, (c) PC-Au film.

2.1.5 Relationship between crystallite size and Vickers hardness (Hv)

Figure 4 shows the results of XRD measurement of the three plating films, (a) AuCo film, (b) DC-Au film, and (c) PC-Au film, using Cu tube (CuKα1: wavelength 1.5405 Å), at 40 kV and 20 mA.

From **Figure 4**, gold peaks of face-centered cubic (FCC) crystal were confirmed in all the samples. The crystallite size D_{hkl} of the (hkl) face (Miller Index) was calculated by the Scherrer equation of the following Eq. (1) [15].

$$D_{hkl} = \frac{K \cdot \lambda}{\beta \cdot \cos\theta} \tag{1}$$

The apparent crystallite size (D_a) was determined using a weighted average of the crystallite sizes from the XRD peaks on each face. In this calculation, the following Eq. (2) was used.

$$D_a = \frac{\sum_{hkl} D_{hkl} \cdot I_{hkl}}{\sum_{hkl} I_{hkl}} = \frac{D_{111} \cdot I_{111} + D_{200} \cdot I_{200} + D_{220} \cdot I_{220} + D_{311} \cdot I_{311}}{I_{111} + I_{200} + I_{220} + I_{311}} \tag{2}$$

As a result, the values of the crystallite size (D_a) from (a) AuCo, (b) DC-Au, and (c) PC-Au films were (a) 19.1 nm, (b) 28.9 nm, and (c) 17.0 nm, respectively. In the original bath, (c) PC-Au film obtained by the pulse electrodeposition has wider peak and smaller Da than that of (b) DC-Au film obtained by the direct current electrodeposition. The reason for these results is related to the fact that the critical radius r_c of the crystal nucleus according to the following Eq. (3) is decreased by pulse electrodeposition with a large overvoltage (η) [16].

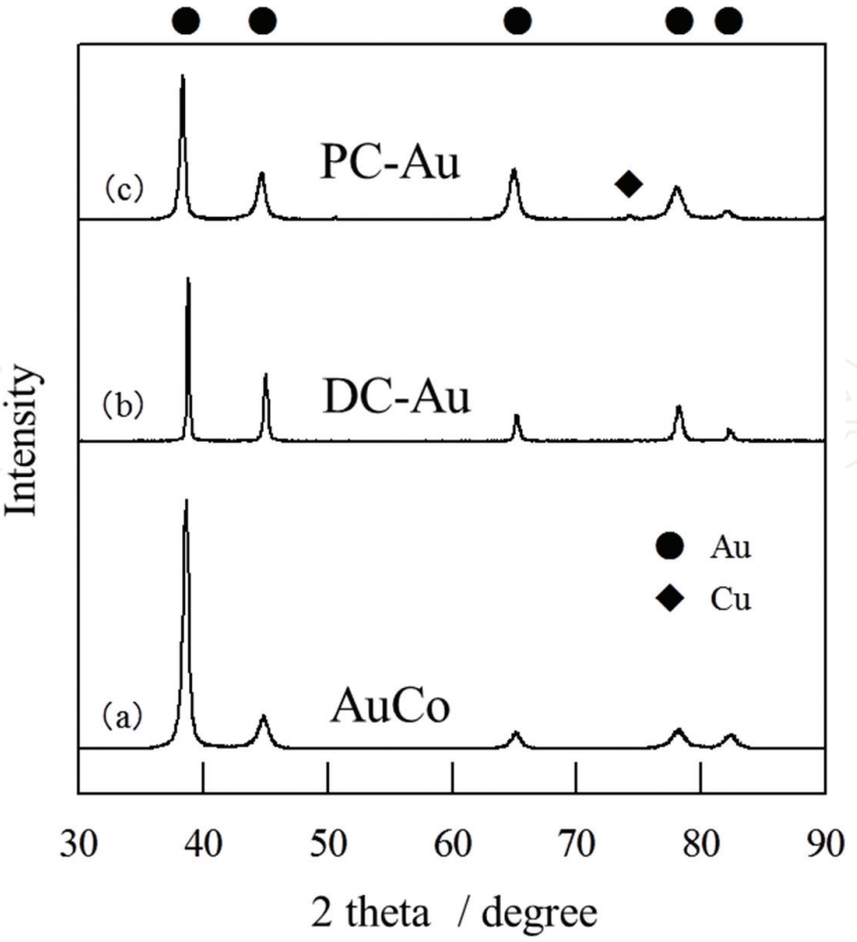

Figure 4.
X-ray diffraction patterns of various Au films; (a) AuCo film, (b) DC-Au film, (c) PC-Au film.

$$r_c = \frac{\gamma \cdot V}{zF \cdot \eta} \tag{3}$$

It is possible to form small crystal nucleus in this case. Here, γ is the intrinsic surface energy, V is the atomic capacity (the volume occupied by 1 g atom in the solid state), z is the valence, F is the Faraday constant, and η is the overvoltage. In general, for metals, the Hall-Petch rule expressed by the following Eq. (4) is established with mechanical yield strength σ [6, 11].

$$\sigma = \sigma_0 + k \cdot d^{-\frac{1}{2}} \tag{4}$$

Here, σ_0 is the intrinsic yield strength (independent of crystal size), k is the constant depending on materials, and d is the crystal size. For the metal film, a proportional relationship is established between the yield strength and the hardness Hv. Paying attention to Eq. (4), the smaller the crystal size is, the harder the metal material is.

Various samples were prepared by changing pulse conditions in the same method, and the relationship between grain size (D_a) from XRD and Hv was as shown in **Figure 5** (Hall-Petch rule).

From the results in **Figure 5**, although the Hv of the pulsed electrodeposition film increases as the crystallite size decreases, the plot tends to decrease from around the critical point ($D_a{}^{-1/2}$ = 0.24). The reason for this is presumed to be the result of the inverse Hall-Petch rule [17–19] that the self-weight collapse occurs in this gold electrodeposition film when the crystallite size becomes too small.

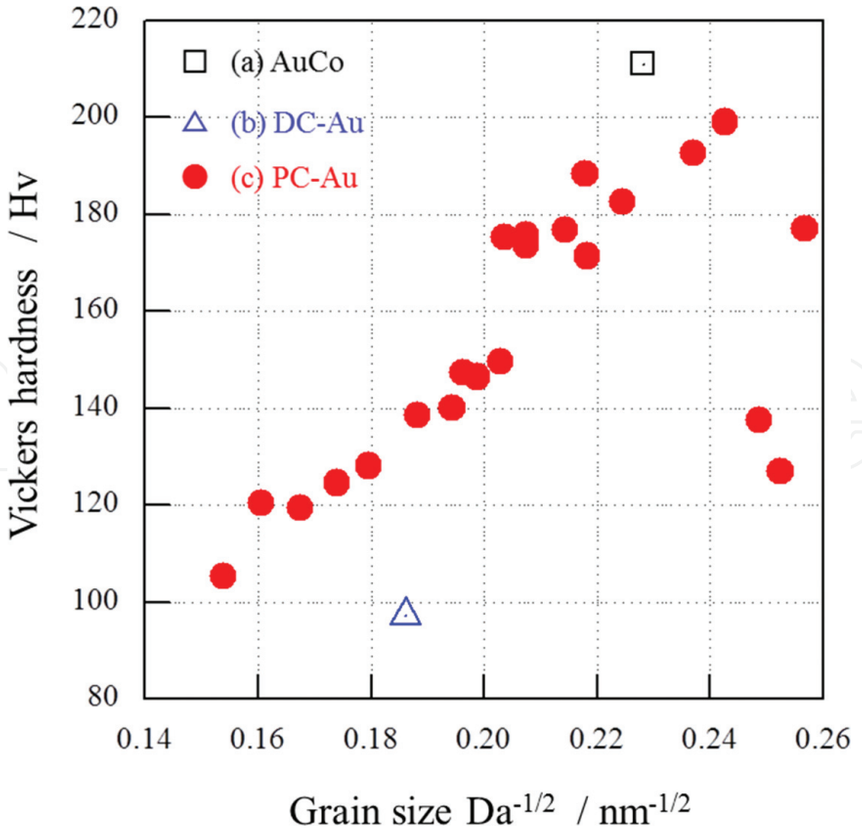

Figure 5.
Relationship between crystallite size (grain size Da) from XRD and Vickers hardness Hv; (a) AuCo film, (b) DC-Au film, (c) PC-Au film.

Therefore, the condition around $D_a^{-1/2}$ = 0.22 (D = 20.7 nm) was selected to form the plated film to obtain appropriate hardness for probe application.

2.1.6 Specific resistance value of plating film

In general, the four probe method of the following Eq. (5) is used as a standard method for measuring the resistivity ρ at RT [20]. Here, the variable t is the plating thickness, and the value (V/I) indicates the resistance value between the measuring terminals.

$$\rho = \frac{\pi t}{\ln 2} \cdot \left(\frac{V}{I}\right) \tag{5}$$

In order to measure the resistivity, the sample plated films were peeled. The resistivity ρ was calculated by the four probe method using the tungsten probe at intervals of 1 mm, and the results are shown in **Table 2** (reference description: crystallite size (D_a), average value of Hv). The plating thickness is obtained by averaging five points as measured by the fluorescent X-ray meter (SFT 3200, SII).

Compared to the resistivity of the commercially available (a) AuCo film, those of both (b) DC-Au film and (c) PC-Au film from the original pure gold plating bath were about 3×10^{-6} mΩ cm lower.

2.1.7 Prototype probe applied with gold plating

In a system in which elastic deformation is predominant, such as 0.1 N < P < 100 N (P is the contact load), the contact resistance R is expressed by the empirical formula of the following Eq. (6) [21, 22]. Here, ρ_1 and ρ_2 are the resistivity

	(a) AuCo	(b) DC-Au	(c) PC-Au
Average of measured resistance values (mΩ)	4.03	2.6	3.2
Deviation of measured resistance value (mΩ)	0.11	0.06	0.92
Average plating thickness (μm)	4.4	3.95	3.44
Specific resistivity ρ (10^{-6} mΩ cm)	8.04	4.65	4.98
Average value of Vickers hardness (Hv)	211	97	199
Apparent crystallite size Da (nm)	19.1	28.9	17

Table 2.
Specific resistivity ρ of samples; (a) AuCo film, (b) DC-Au film, (c) PC-Au film (reference description: crystallite size Da, average value of Vickers hardness).

values of two materials in contact, H is the Brinell hardness, and P is the contact load.

$$R = 140 \cdot \frac{\rho_1 + \rho_2}{2} \cdot \sqrt{\frac{H}{P}} \tag{6}$$

It is suggested that the contact resistance can be lowered by the decrease of the resistivity proportional to its value. Utilizing this, the pulsed hard pure gold plating film was applied to the parts of the probe. Using two types of plated film probes, (a) AuCo film (conventional product) from commercial cyanide bath and (c) PC-Au film (fabricated product) from original bath, the results of the durability comparison during the contact resistance of 100,000 times are shown in **Figure 6**. In **Figure 6**, the vertical axis represents the contact resistance value [mΩ] of the probe; (a) AuCo plating and (c) PC-Au plating, and the horizontal axis represents every 1000 durability measurement times. The bar is maximum and minimum values at every 1000 times measurement, and the average values were plotted.

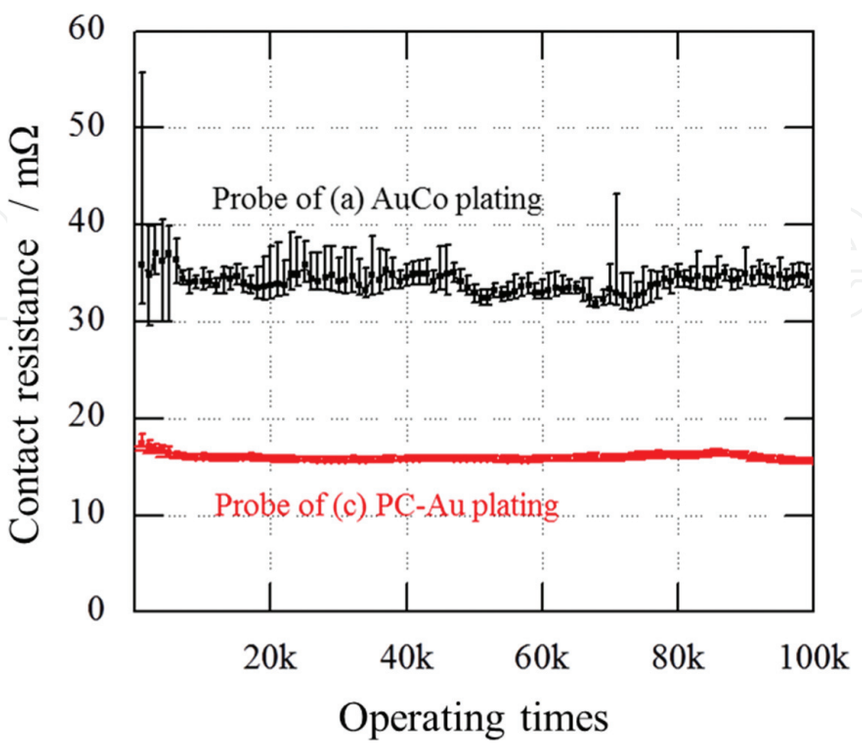

Figure 6.
The durability about the contact resistance of 100,000 times; the probe of (a) AuCo plating and (c) PC-Au plating.

Calculating the average value of the contact resistance, (a) the resistance of the conventional product probe was 32.6 mΩ (deviation 2.07), and (c) that of the fabricated product probe was 21.6 mΩ (deviation 0.80). This fabricated probe has an advantage that the contact resistance value decreases by 11 mΩ and its variation is low, and improvement of electrical contact characteristics could be realized.

2.2 Gold-CNT composite plating

Carbon materials have attracted attention for a long time due to their characteristic structural, electronic, thermal, chemical, mechanical properties [23]. Since the discovery of carbon nanotube (CNT) [24, 25], great number of fundamental and technological research on CNT has been developed [26]. CNT is characterized by small diameter and high aspect ratio with outstanding mechanical strength, flexibility, high electrical conductivity and chemical stability [27].

For instance, material-CNT composites as a lightweight and high strength material have been actively studied [28–32]. Recently, CNT's application of seawater desalination has progressed in Shinshu University and has been drawing attention [33]. In general, the hydrophilic property at the interface and the difference in specific gravity between a metal matrix and filled CNTs make it difficult to fabricate a metal-CNT composite film with uniformly distributed CNTs and a good tribological behavior. Metal-CNT composite films have been fabricated [34–37], using various types of metals (Ni, Cu and Ag) by composite plating [38–44]. However, the pH levels of plating baths, being on the acidic side, are low. There are very few reports about the fabrication of a CNT composite plating film under the basic condition. Moreover, recently used industrial electric contacts, for example, a probe for inspecting parts of a semiconductor package, have encountered a drawback due to their adhesion and increase in resistivity after repeated use. Thus, a non-adhesive plating material for connector application is strongly required.

In this section, to develop a new composite material for next-generation electric contact applications, an Au-CNT composite plating film was fabricated by electrodeposition [40]. An effective additive was added into a non-cyanide CNT plating solution, affording the formation of an Au-CNT composite film in a basic solvent by an environmentally friendly method.

2.2.1 Carbon nanotube (CNT) and gold plating bath

A vapor-grown carbon fiber (VGCF; Showa Denko) which is one type of multiwalled CNTs, was used in this study. An Au-CNT plating bath was prepared by adding 0.05 M $Na_3Au(SO_3)_2$, 0.5 M Na_2SO_3, 100 pp. 2,2′-dipyridyl, and 0.2 g/l VGCF into ion-exchanged water. Moreover, 0.1 g/l trimethyl stearyl ammonium chloride ($C_{21}H_{46}ClN$) was added into the above solution. The mixture was stirred using an ultrasonic agitator (28 kHz) for 2 h. The volume of the plating bath was 100 cm^3. The plating was performed at 60°C and pH 8 using a magnetic stirring agitator. The current density was 50 A/m^2 and a Pt-plated Ti mesh was used as the anode [8]. A copper (Cu) board with an exposed area of 200 mm^2 (10 × 20 mm^2) was used as the substrate. The Cu substrate was plated using a Ni-P amorphous alloyed layer with a thickness of 3 mm. A Ni-P plating bath is a commercially available plating solution (Meltex). Before plating, the substrate was pretreated by alkali degreasing and acid treatment. For comparison, an Au plating film was prepared using an Au plating bath without adding CNTs. FE-SEM equipped with energy-dispersive X-ray spectroscope (EDX; JED-2300F, JEOL) was used to study the surface morphology and CNT content of the fabricated plating films. Hv was measured using a dynamic hardness tester (DUH-201, Shimadzu). A diamond

indenter was vertically employed with a test load of 0.098 N, a load speed of 6.6 mN/s, and a hold time of 20 s at RT. The intrinsic resistance of the fabricated plating films was determined by a four-point probe method. Tungsten (W) probes were used with a probe spacing of 1 mm. Tribological properties were measured using a ball-on-plate-type reciprocating friction abrasion test machine (MMS-2419, Nissho-EW). A brass ball (8 mm in diameter) plated with 4.5 μm Ni-P and 1 μm hard-Au layers, was used as the counter surface. The test was repeatedly conducted in 50 cycles at a load of 0.5 N, a sliding length of 2 mm, a sliding speed of 0.5 mm/s at RT. The test was performed under ambient conditions without any lubricants. During the test, the friction coefficient was measured continuously using a load tester.

2.2.2 Gold-CNT composite plating film

The fabricated Au-CNT composite film appeared to be relatively black. **Figure 7 (a)** and **(b)** shows SEM images of the fabricated Au-CNT composite film and the Au film, respectively.

CNTs were tangled with the Au matrix and protruded from the matrix surface. The surface morphology of the Au-CNT composite film was relatively rough owing to the existence of many voids. It was previously reported that, in the composite film, metal is easily separated at the CNT apex and defects of CNTs. Before CNTs are entirely coated, the plating process is promoted at the apex or defects of CNTs, resulting in the formation of voids in the deposited film [34]. The result of EDX analysis indicated that the content of CNTs in the Au plating film was about 4 mass %. In the plating process, CNTs could not be homogeneously dissolved in the solution without $C_{21}H_{46}ClN$ even if it had been mechanically stirred for 48 h, and consequently, the plating bath could not be prepared. From the above results, $C_{21}H_{46}ClN$ was found to be an effective additive for Au-CNT composite film fabrication using a non-cyanide bath, which is an environmentally friendly method.

2.2.3 Gold plating bath and zeta potential

The mechanism of the eutectoid composition of the Au-CNT composite film is assumed to be based on the deposition of CNTs by electrophoresis. Normally, the zeta potential of CNTs decreases and easily becomes negative when the solution becomes basic [45, 46]. Although CNTs are modified by N-doping or heat treatment, their zeta potential becomes negative at a basic pH of 8 [47, 48]. Since the CNTs repulsed by the cathode during reduction react, it is difficult to combine CNTs in a basic solution. At this stage, although the role of the additive has not yet

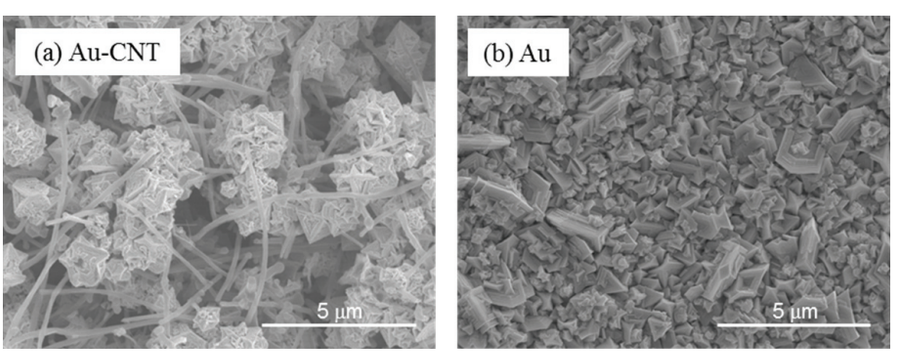

Figure 7.
SEM images of the surface sample; (a) the fabricated Au-CNT composite film, (b) Au film.

been clearly elucidated, the results obtained in this study apparently show that the additive is important for Au-CNT composite film fabrication.

Figure 8 shows the VGCF zeta potential of 0.05 g/L under various potential of hydrogen (pH) in three solutions; (a) conventional dispersant of 0.5 mM in water, (b) fabricated dispersant ($C_{21}H_{46}ClN$) of 0.5 mM in water, (c) plating solution diluted 20 times.

The hydrophobicity of the additive is likely to effectively provide a positive zeta potential for CNTs. This was also evidenced in the plating process. The zeta potential of CNTs was found to be positive in the solution, and consequently, CNTs with a positive zeta potential were attracted toward the plating cathode.

2.2.4 Hardness and electrical properties of Au-CNT composite film

Table 3 shows the Hv and resistivity of the Au-CNT composite film and the Au film, respectively. The Hv is the average measured at 10 points. In general, to measure the Hv accurately, film thickness is required to be 10 times higher than the depth of the indenter pressed into the film. Thus, it should be noted that the measured value includes the substrate effect.

The Hv of the Au-CNT composite film and the Au film were Hv 133 and Hv 95, respectively. The fabricated Au-CNT composite film was harder than the Au film by 1.4 times.

For intrinsic resistance measurement, while the film thickness is sufficiently small compared with the probe spacing, the intrinsic resistivity ρ can be expressed by $\rho = (\pi t/\ln 2)/(V/I)$ [20], where value t is the average film thickness measured at

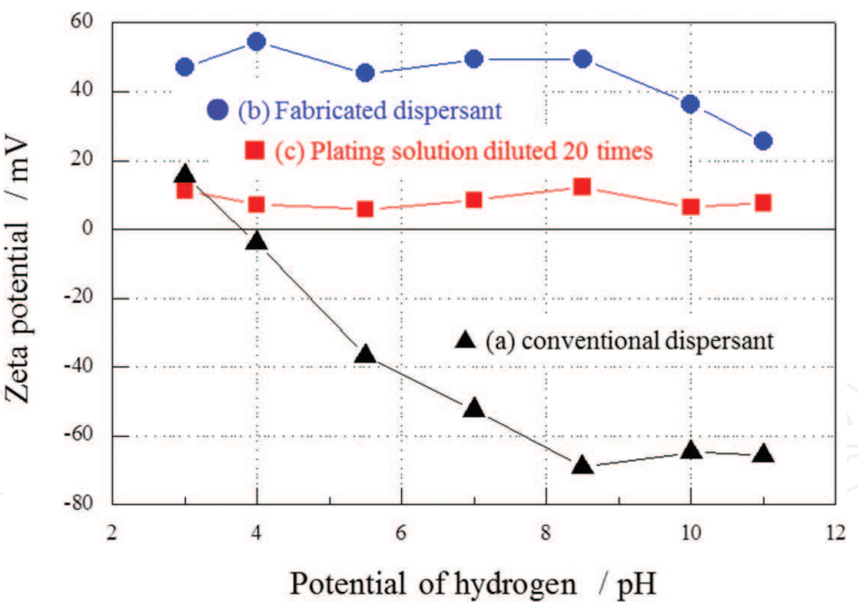

Figure 8.
The VGCF zeta potential of 0.05 g/L under various potential of hydrogen (pH) in three solutions; (a) conventional dispersant of 0.0005 M in water, (b) fabricated dispersant (C21H46ClN) of 0.0005 M in water, and (c) plating solution diluted 20 times.

	Vickers hardness (Hv)	Resistivity (10^{-6} mΩ cm)
Au-CNT composite film	133	5.63
Au plating film	95	4.65

Table 3.
The Vickers hardness and resistivity of the Au-CNT composite film and the Au film.

five points by X-ray fluorescence analysis (SFT3200, SII), and (V/I) is the average resistance of the thin film measured at three points. The resistivity of the Au-CNT composite film and the Au film were 5.6 and 4.7 × 10^{-6} mΩ cm, respectively. The fabricated Au-CNT composite film showed a higher resistivity than the Au film by 1.2 times. The voids and the interface between Au and CNTs are likely attributed to the Vickers hardness and the resistivity.

2.2.5 Friction coefficients of the Au-CNT composite film

Figure 9 shows the friction coefficients of the Au-CNT composite film and the Au film, as a function of sliding length against Sn ball of 8 mm diameter.

In the case of the Au-CNT composite film, the friction coefficient gradually decreased toward the sliding length. After the test, at a total sliding length of 200 mm (50 repeated cycles), the friction coefficient was 0.28. On the other hand, in the case of the Au film, the friction coefficient increased to 0.58 and gradually decreased at a sliding length of 130 mm. The Au-CNT composite film showed a lower friction coefficient than the Au film.

Figure 10(a) and **(b)** shows SEM images of the Au-CNT composite film and the Au film after the wear test, respectively.

The worn area of (b) the Au film was relatively large compared with that of (a) the Au-CNT composite film. The track with a width of approximately 200 mm was

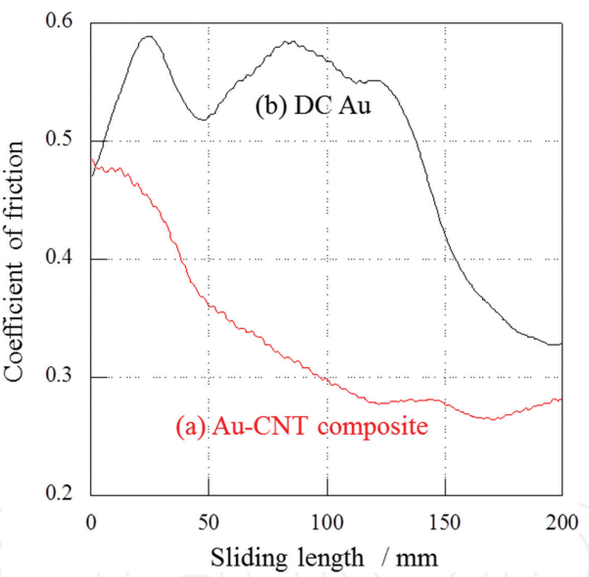

Figure 9.
The friction coefficient of (a) the Au-CNT composite film and (b) the Au film, as a function of sliding length against Sn ball of 8 mm diameter.

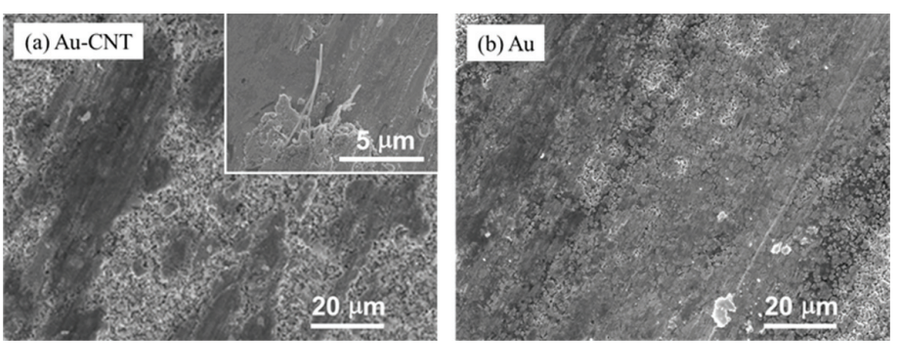

Figure 10.
SEM images of (a) the Au-CNT composite film and (b) the Au film after the wear test.

found on the surface of the Au film. The entire surface of the worn area of the Au film was damaged, while that of the Au-CNT composite film was partly damaged. CNTs still remained in the worn area of the Au-CNT composite film, lying transversely [**Figure 10(a)** inset]. Adhesive wear is one of the friction phenomena. The smaller the surface area, the weaker the force of the adhesion shear [49]. The small contact area and transversely lying CNTs seem to contribute to the low friction coefficient.

3. Conclusions

To summarize, a pure-gold plated film with nano-order crystals was fabricated by devising a pulse electrolysis method using a non-cyanide bath. As a result of confirming their structure with FE-SEM or XRD, although refinement of this crystal showed an increase in hardness according to Hall-Petch rule, this law did not hold in the range smaller than around Da = 20 nm, and on the contrary it showed a decrease in hardness. By controlling a crystallite size (around Da = 21 nm) where the hardness does not decrease, the fabricated pure gold plating film without alloying maintains a moderate hardness (Hv = 199: Hv = 210 with AuCo film), its specific resistance (5×10^{-6} mΩ cm: 8×10^{-6} mΩ cm with AuCo film) than the conventional hard gold plating film. By applying the developed plating film to the probe, the contact resistance value of the repeated test could be reduced by about 11 mΩ, be achieving high performance with low variation. Conventionally, non-cyanic plating baths have lower life and stability compared to cyanide baths, and this is also a problem in the developed plating baths. However, compared to conventional AuCo plating, the fabricated hard pure gold plating has superiority in environmentality and workability with non-cyan, reliability of electric contact (reduction in contact resistance, stability of repeated variation).

In summary of the second film, an Au-CNT composite plating film was fabricated by electrodeposition. A non-cyanide Au-CNT composite plating film was successfully formed by adding an effective additive, at alkaline environment. This was presumed to relate the zeta potential. The Au-CNT composite film is advantageous over the Au plating film in terms of a high hardness and a low friction coefficient. Thus, the Au-CNT composite film along with the desired method and the precise control of the content and orientation of CNTs are expected to make CNTs as promising material of sliding electric contacts, such as connectors.

In view of the application of contact materials used for MEMS, two methods of gold plating were introduced. In the society where miniaturization is advancing, the role of electrical contacts has also grown. Gold as a contact material will become more important. As described above, the advantage and potential of the new gold plating were confirmed, but there is still room for improvement in terms of performance. In addition, issues such as economical cost, safety of the use side, system construction for sustainable society formation (recycling) remain. Technological progress in the future is strongly expected.

Acknowledgements

This work was supported by MEXT Cluster brochure (Nagano Prefecture region). We express our appreciation to Prof. Morinobu Endo of Shinshu University for his great support and fruitful discussion. We also thank to Dr. Kenji Takeuchi and Dr. Noboru Akuzawa of Shinshu University, Dr. Winadda Wongwiriyapan of King Mongkut's Institute of Technology Ladkrabang, Prof. Feng Wang of Beijing University of Chemical Technology, for their kind advices.

Author details

Masatsugu Fujishige and Susumu Arai*
Shinshu University, Nagano, Japan

*Address all correspondence to: fshige@shinshu-u.ac.jp

IntechOpen

References

[1] Feynman RP. There's plenty of room at the bottom. Journal of Microelectromechanical Systems. 1992; **1**(1):60-66

[2] Gardner JW, Varadan VK, Awadelkarim OO. Microsensors, MEMS, and Smart Devices. John Wiley & Sons, Ltd; 2001. p. 5. https://www.wiley.com/en-us/Microsensors%2C+MEMS%2C+and+Smart+Devices-p-9780471861096

[3] Zhang R, Pian H, Santosh M, Zhang S. The history and economics of gold mining in China. Ore Geology Reviews. 2015;**65**:718-727

[4] James TGH. Gold technology in ancient Egypt: Mastery of metalworking method. Gold Bulletin. 1972;**5**(2):38-42

[5] Klemm D, Klemm R, Murr A. Gold of the Pharaohs—6000 years of gold mining in Egypt and Nubia. African Earth Sciences. 2001;**33**:643-659

[6] Nishikawa S. Gold, Grain Size and Yield Stress, Shinban Kinzokukougaku Nyumon. Agune Gijyutsu Center; 2001. pp. 150-500 (in Japanese)

[7] Fujishige M, Arai S, Wang F, Ushiyama M, Park KC, Takeuchi K, et al. Improvement of electric contact in probes by nanocrystallization-enhanced hardening of pure gold plating films. IEICE Transactions C. 2006;**J92-C**(6): 218-224

[8] Hosokawa K. Application of pulse electrodeposition. Kinzoku Hyomengijyutsu. 1988;**39**(4):156-161 (in Japanese)

[9] Cheh HY. Electrodeposition of gold by pulsed current. Journal of the Electrochemical Society. 1971;**118**(4): 551-557

[10] Lan LT, Ohno I, Haruyama S. Nucleation and growth in pulse plating. Denki Kagaku. 1983;**51**(1):167-168 (in Japanese)

[11] Nieh TG, Wang JG. Hall-Petch relationship in nanocrystalline Ni and Be-B alloys. Intermetallics. 2005;**13**: 377-385

[12] Fujishige M, Arai S, Wang F, Endo M, Ushiyama M, Makizaki S. Non-cyan hard Au plating for probe. In: Reports of the 114th Annual Meeting (Hokkaido University) of SFSJ. The Surface Finishing Society of Japan; 2006. pp. 58-59 (in Japanese)

[13] Kagaya Y, Honma H. Gold plating from gold sulfite complex. Journal of the Surface Finishing Society of Japan. 1993; **44**(7):638-642 (in Japanese)

[14] Tamai T. Effect of humidity in the atmosphere on electrical contact characteristics. IEICE Technical Report. 2006;**105**(604):13-18

[15] Analysis Center in Rigaku Corporation. X-ray Diffraction Guide. Rigaku Corporation.; 1981. pp. 75-79. NCID: BA67145761 (in Japanese)

[16] Haruyama S. Mechanism and speed of electrodeposition. In: Electrochemistry for Surface Engineers. Maruzen Co; 2005. pp. 132-134. ISBN: 4-621-07573-X C 3058 Printed in Japan

[17] Takeuchi S. The mechanism of the inverse Hall-Petch relation of nanocrystals. Scripta Materialia. 2001; **44**:1483-1487

[18] Fan GJ, Choo H, Liaw PK, Lavernia EJ. A model for the inverse Hall-Petch relation of nanocrystalline materials. Materials Science and Engineering A. 2005;**409**:243-248

[19] Song HW, Guo SR, Hu ZQ. A coherent polycrystal model for the inverse Hall-Petch relation in nanocrystalline materials. Nanostructured Materials. 1999;**11**(2): 203-210

[20] Okada T. Electron conduction and current magnetic effect. In: Electrical Properties—Laboratory Physics Course. Kyoritsu Shuppan Co., Ltd.; 1977. pp. 57-61.ISBN-10: 4320030710; ISBN-13: 978-4320030718

[21] Holm R. Stationary Contacts, Electric Contacts. 4th ed. Springer-Verlag; 1967. pp. 40-47. ISBN: 9783662066881 3662066882 9783642057083 364205708X; OCLC No.: 652351662. https://www.springer.com/la/book/9783540038757

[22] Tamai T. Friction and contact resistance through true contact interface. IEICE Technical Report. 2005; **105**(412):7-12

[23] Dresselhaus MS, Dresselhaus G, Eklund PC. Science of Fullerenes and Carbon Nanotubes. New York: Academic Press, Inc; 1996

[24] Oberlin A, Endo M, Koyama T. Filamentous growth of carbon through benzene decomposition. Journal of Crystal Growth. 1976;**32**:335-349

[25] Iijima S. Helical microtubules of graphitic carbon. Nature. 1991;**354**: 56-58

[26] Endo M, Hayashi T, Kim YA, Muramatsu H. Development and application of carbon nanotubes. Japanese Journal of Applied Physics. 2006;**45**(6A):4883-4892

[27] Dresselhaus MS, Dresselhaus G, Avouris P. Carbon Nanotubes; Synthesis, Structure, Properties and Application. New York: Springer; 2001

[28] Martinez-Sanchez R, Estrada-Guel I, Miki-Yoshida M, Antunez-Flores W, Santos-Beltran A, Barajas-Villaruel I. Novel composites aluminum-multi-walled carbon nano-tubes. Microscopy and Microanalysis. 2005;**11**:1738-1739

[29] George R, Kashyap KT, Rahul R, Yamdagni S. Strengthening in carbon nanotubes/aluminium (CNT/Al) composites. Scripta Materialia. 2005;**53**: 1159-1163

[30] Noguchi T, Magario A, Fukazawa S, Shimizu S, Beppu J, Seki M. Carbon nanotube/aluminium composites with uniform dispersion. Materials Transactions. 2004;**45**(2):602-604

[31] Endo M, Noguchi T, Ito M, Takeuchi K, Hayashi T, Kim YA, et al. Extreme-performance rubber nanocomposites for probing and excavating deep oil resources using multi-walled carbon nanotubes. Advanced Functional Materials. 2008; **18**:3403-3409

[32] Takeuchi K, Noguchi T, Ueki H, Niihara K, Sugiura T, Inukai S, et al. Improvement in characteristics of natural rubber nanocomposite by surface modification of multi-walled carbon nanotubes. Journal of Physics and Chemistry of Solids. 2015;**80**:84-90

[33] Inukai S, Cruz-Silva R, Ortiz-Medina J, Morelos-Gomez A, Takeuchi K, Hayashi T, et al. High-performance multi-functional reverse osmosis membranes obtained by carbon nanotube-polyamide nanocomposite. Scientific Reports. 2015;**5**(13562):1-10

[34] Guglielmi N. Kinetics of the deposition of inert particles from electrolytic baths. Journal of the Electrochemical Society. 1972;**119**:1009

[35] Musiani M. Electrodeposition of composites: An expanding subject in electrochemical materials science.

Electrochimica Acta. 2000;**45**: 3397-3402

[36] Low CTJ, Wills RGA, Walsh FC. Electrodeposition of composite coatings containing nanoparticles in a metal deposit. Surface and Coating Technology. 2006;**201**(1–2):371-383

[37] Hovestad A, Janssen LJJ. Electrochemical codeposition of inert particles in a metallic matrix. Journal of Applied Electrochemistry. 1995;**25**: 519-527

[38] Arai S, Endo M. Various carbon nanofiber-copper composite films prepared by electrodeposition. Electrochemistry Communications. 2005;**7**:19-22

[39] Arai S, Endo M, Kaneko N. Ni-deposited multi-walled carbon nanotubes by electrodeposition. Carbon. 2004;**42**:641-644

[40] Arai S, Fujimori A, Murai M, Endo M. Excellent solid lubrication of electrodeposited nickel-multiwalled carbon nanotube composite films. Materials Letters. 2008;**62**:3545-3548

[41] Fujishige M, Sekino M, Fujisawa K, Morimoto S, Takeuchi K, Arai S, et al. Electric contact characteristic under low load of silver–carbon nanotube composite plating film corroded using H_2S gas. Applied Physics Express. 2010; **3**:065801

[42] Arai S, Osaki T, Hirota M, Uejima M. Fabrication of copper/single-walled carbon nanotube composite film with homogeneously dispersed nanotubes by electroless deposition. Materials Today Communications. 2016; **7**:101-107

[43] Arai S, Kanazawa T. Electroless deposition of Cu/multiwalled carbon nanotube composite films with improved frictional properties. Journal of Solid State Science and Technology. 2014;**3**(6):201-206

[44] Fujishige M, Wongwiriyapan W, Wang F, Park KC, Takeuchi K, Arai S, et al. Gold-carbon nanotube composite plating film deposited using non-cyanide bath. Japanese Journal of Applied Physics. 2009;**48**:070217

[45] Lu C, Chiu H. Adsorption of zinc(II) from water with purified carbon nanotubes. Chemical Engineering Science. 2006;**61**:1138-1145

[46] Yang K, Xing B. Adsorption of fulvic acid by carbon nanotubes from water. Environmental Pollution. 2009; **157**:1095-1100

[47] Lu C, Su F. Adsorption of natural organic matter by carbon nanotubes. Separation and Purification Technology. 2007;**58**:113-121

[48] Amadou J, Chizari K, Houlle M, Janowska I, Ersen O, Begin D, et al. N-doped carbon nanotubes for liquid-phase CC bond hydrogenation. Catalysis Today. 2008;**138**:62-68

[49] Kimura Y, Okabe H. Tribology-gairon. Tokyo: Yokendo; 1985. p. 34 (in Japanese)

IntechOpen